4.2 RECENT PROGRESS IN THE FABRICATION AND CHARACTERIZATION OF DUCTILE-PHASE-TOUGHENED TUNGSTEN LAMINATES FOR PLASMA-FACING MATERIALS—K. H. Cunningham, G. R. Odette, K. Fields, D. Gragg, T. Yamamoto, and F. W. Zok (University of California, Santa Barbara), C. H. Henager, Jr., R. J. Kurtz, T. J. Roosendaal, and B. A. Borlaug (Pacific Northwest National Laboratory)

OBJECTIVE

The objective of this study is to develop ductile-phase-toughened tungsten composites as candidates for plasma-facing components in future fusion reactors.

SUMMARY

A promising approach to increasing the fracture toughness of W-alloys is ductile-phase toughening (DPT). A ductile phase reinforcement in a brittle matrix increases toughness primarily by crack bridging. A W-Cu laminate was fabricated and the properties of the constituent metals were characterized along with those for the composite. Development of a design model for large-scale crack bridging continued.

PROGRESS AND STATUS

Introduction

Background information and previous progress have been discussed in earlier semi-annual reports [1-3].

Experimental Procedure

Brazed W-Cu Laminate

Diffusion bonding of W to Cu via hot pressing was found to be inconsistent, so brazing W plates with thin layers of Cu was explored. Lapped 0.85 x 50 x 50 mm W plates were stacked alternating with 75-µm Cu foils, and clamped with stainless steel wire. The layup was heated in an Ar-5%H_2 environment to 1113 °C at 15 °C/min and held for 6 s before cooling. Notched three-point bend bars were fabricated from both the as-received W plate and the W-Cu laminate. The dimensions of the W bars were 22 x 4.65 x 0.85 mm, and the W-Cu bars were 21 x 4.65 x 2.125 mm. The notch depth was nominally 0.93 mm. All specimens were identified with respect to the rolling direction of the W plate: the “L” and “T” labels indicate the crack propagation direction was parallel (L) or perpendicular (T) to the rolling direction. Laminate specimens were also separated into “edge” and “face” orientations, where the crack propagation direction was normal to the edge or face of W and Cu layers, respectively.

Characterization of the fracture toughness of the W plate in the L and T orientations is needed to establish a constituent baseline for comparison with the laminate fracture resistance. Notched W bend bars were compression pre-cracked by standing them upright in a load frame with the span along the fatigue loading direction as shown in Figure 1. The specimens were compression-compression fatigued at 20 Hz and the crack length was observed at intervals of 10,000 cycles until reaching a length of approximately a/W=0.3. The specimens were then tested in three-point bending and toughness values were calculated following ASTM E399-12. The pre-crack depth was measured by applying a dye penetrant to the sample prior to testing and subsequently observing the marked area.

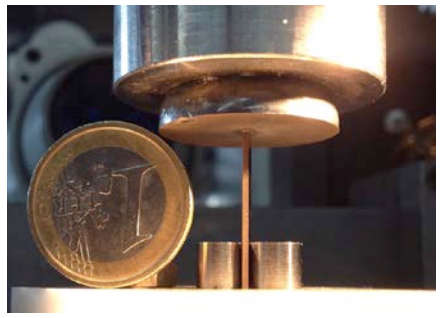

Figure 1. Photograph of end-on compression fatigue setup for W bend bars. A steel clip is used to help stand the specimen upright.

The W-Cu laminate bars were fatigued in three-point bending to attempt to develop a precrack, without success. The current test data from several specimens comes from bend bars with a rounded EDM-cut notch, with an average radius of 158 μm. Some precracking attemps resulted in the laminate specimens breaking to roughly a/W=0.9. This allowed investigation of the Cu bridging phase. Other specimens were tested in three-point flexure with a crosshead displacement rate of 0.1 mm/min.

Large-Scale Crack Bridging Code

In parallel with laminate fabrication efforts, we have been developing a code to predict resistance and load-displacement curves for ductile-phase-toughened composites for different geometries and composite architectures. The code is adapted from work by Odette and Chao [4, 5] on TiAl-TiNb laminates. The approach of the code is to calculate the shape of the crack from the applied load (opening) and the distributed bridging stresses along the crack face (closing) using Castigliano's Theorem and stress intensity solutions from Tada. An iterative calculation reaches a self-consistent solution by matching the stress-displacement function of the reinforcing phase with those calculated for the crack opening displacement profile. The code predicts both the fracture resistance and load-displacement curves. Note the p-Δ curves are equivalent to stress-strain curves in cracked bodies, hence they provide engineering measures of composite strength and ductility. A description of the algorithm sequence is shown below, and Figure 2 shows the model of a three-point bend specimen.

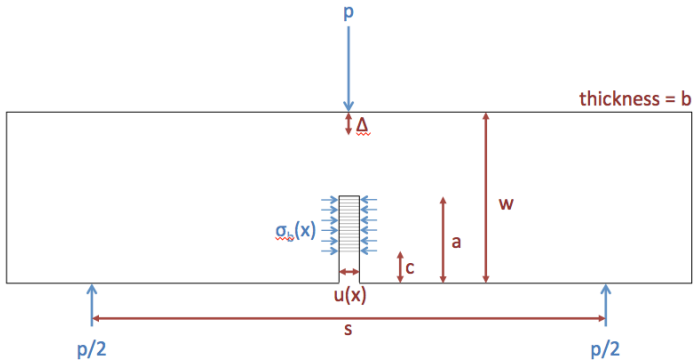

Figure 2. Schematic of the three-point bend specimen modeled in the bridging code. Note that the x-direction is the crack propagation direction with a range of 0 to a. Specimen dimensions are shown in red and stresses in blue.

- Input information
  - Specimen and crack dimensions
  - Matrix properties (K_m, E, v)
  - Reinforcement stress-displacement law $\sigma_b(u)$

- Iterative calculation of crack face displacements and stresses
  - Assume a bridge stress distribution $\sigma_b^*(x)$

- Calculate the stress intensity factor (K_I) for a specified crack length (a) and remote load (p)
- Calculate the stress intensity reduction at the crack tip due to the σ_b*(x) distribution
- Calculate the applied increased stress intensity needed to advance the crack at $K_{tip} = K_m$
- Calculate the net crack face displacement distribution u*(x) due to the applied K_I (opening) and the bridging zone traction stress distribution σ_b*(x) (closing)
- Estimate a new stress distribution using a specified ductile ligament stress-displacement function $\sigma_b(u)$ and the calculated u*(x) as described in the next two steps
- Compare the σ_b*(x) distribution used initially with $\sigma_b[u(x)]$ and compute the difference $\varepsilon(x)$
- Set $\sigma_b[u(x)]$ to a new σ_b*(x) and repeat the above calculations, iterating until σ_b*(x) = $\sigma_b[u(x)]$ and thus $\varepsilon(x) \approx 0$ for all x.
- Use the expressions in Tada to calculate the corresponding load-point displacement (Δ)
- Increase the crack length a by a small increment (da) and repeat to calculate the resistance curve $K_I(a)$ and load-displacement curve $p(\Delta)$

Results

W Plates and Brazed W-Cu Laminate

Fracture toughness values of the W plate in both orientations are shown in Table 1. The average toughness values in the L and T directions are 13.06 and 20.90 MPa $m^{0.5}$, respectively. Bend testing on the W-Cu laminate did not show pseudo-ductile behavior, but crack bridging did occur. In Figure 3, the dye penetrant on the fracture surface of the broken specimen indicates that when the specimen was still intact with an a/W ≈ 0.9, the Cu the reinforcement was bridging the crack. An increase in load-bearing capacity and fracture resistance is not seen in these specimens because the applied stress intensity needed to grow a sharp crack from the blunt notch tip was greater than that needed to unstably propagate a sharp dynamic crack to a/w=0.9, since the corresponding crack opening profile does not activate a significant bridging traction. Using the compression precracking method on the W-Cu samples should allow for stable crack growth and characterization of the corresponding resistance curves.

Table 1. Measured fracture toughness values for pure W three-point bend specimens. Test dimensions are 20.5 x 4.65 x 0.85 mm.

Specimen	a/W	Load (N)	K_{IC} (MPa $m^{0.5}$)
L2	0.26	101.60	10.52
L5	0.28	98.96	10.74
L6	0.33	120.70	14.70
L7	0.27	129.73	13.60
L8	0.31	135.54	15.73
T2	0.27	195.29	20.46
T3	0.30	190.81	21.52
T6	0.27	199.55	20.85
T8	0.26	200.55	20.75

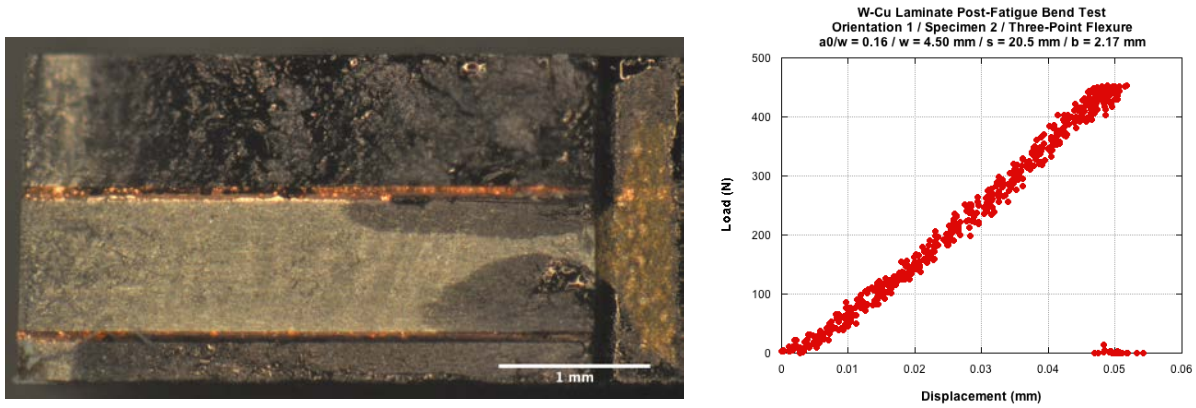

Figure 3. Left: a representative fracture surface of edge specimen 1 marked with dye penetrant. Notch is on the right side of image. Specimen was broken to a/W = 0.9, as marked by the dye. Lack of penetration through Cu layers indicates Cu was bridging the crack. Right: a representative load-displacement curve for edge specimen 2 indicates brittle failure.

Large-Scale Crack Bridging Code

The large-scale crack bridging code results were compared the previous work of Odette and Chao [4, 5], since that work was validated experimentally. Examples of the crack shape and accompanying stress distribution for an arbitrary reinforcement in W are shown in Figure 4. Figure 5 shows resistance curves and load-displacement curves calculated for three different bridging stress-displacement functions, indicated by color. The new resistance curve calculations (points) compare very well with the previous results (lines) but the p-Δ predictions are only consistent up to nearly the peak load. After the peak load, the load-point displacement is under-predicted with respect to the previous results. The calculation converges quickly when modeling specimens in the edge orientation because the reinforcement is continuous in the direction of crack propagation. The presence of discontinuities in the reinforcement phase with respect to the crack propagation direction results in convergence issues when modeling the face orientation.

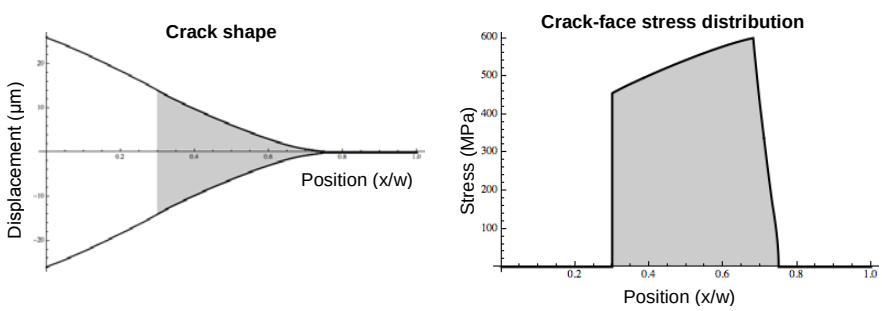

Figure 4. Example output from large-scale bridging code. Left: crack shape with bridging zone shaded. Right: crack-face stress distribution.

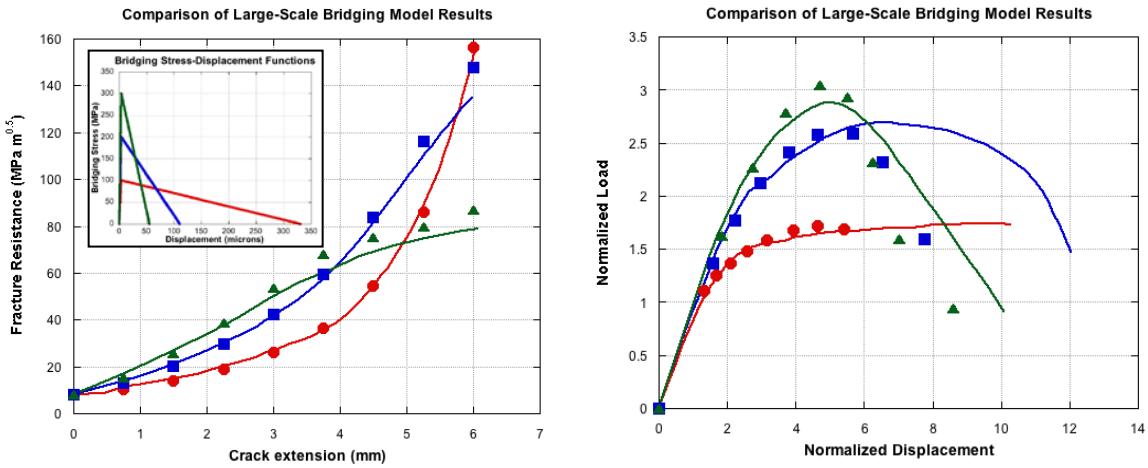

Figure 5. Experimentally-verified models (lines) [4] compared with current models (points) for identical initial conditions, modeling a TiAl-TiNb laminate. Left: comparison of resistance curves. Right: comparison of load-displacement curves. Values are normalized by the load capacity and displacement at fracture of a non- reinforced test specimen. Inset at left: bridging stress-displacement functions corresponding to the colors in each plot.

Ongoing and Future Work

Laminate testing and large scale bridging code development will continue. The laminate studies will include a variety of ductile reinforcement phases as alternatives to Cu. New methods will be developed to pre-crack the laminates and to utilize the data from the notched bars.

References

[1] K. H. Cunningham, K. Fields, D. Gragg, F. W. Zok, C. H. Henager, Jr, R. J. Kurtz, and T. Roosendaal, Recent Progress in the Development of Ductile-Phase Toughened Tungsten for Plasma-Facing Materials, in DOE/ER-0313/54 - Volume 54, Semiannual Progress Report, June 30, 2013. 2013, US DOE: ORNL, TN.

[2] C. H. Henager, Jr, R. J. Kurtz, T. J. Roosendaal, B. A. Borlaug, G. R. Odette, K. H. Cunningham, K. Fields, D. Gragg, and F. W. Zok, Recent Progress in the Development of Ductile-Phase Toughened Tungsten for Plasma-Facing Materials, in DOE/ER-0313/55 - Volume 55, Semiannual Progress Report, Dec. 31, 2013. 2013, US DOE: ORNL, TN.

[3] K. H. Cunningham, G. R. Odette, K. Fields, D. Gragg, F. W. Zok, C. H. Henager, Jr., R. J. Kurtz, T. J. Roosendaal, and B. A. Borlaug, Recent Progress in the Fabrication and Characterization of Ductile-Phase-Toughened Tungsten Composites For Plasma-Facing Materials, in DOE/ER-0313/56 - Volume 56, Semiannual Progress Report, Jun. 30, 2014. 2014, US DOE: ORNL, TN.

[4] G. R. Odette, B. L. Chao, J. W. Sheckherd, and G. E. Lucas. Acta Metall. Mater. 40-9 (1992) 2381-2389.

[5] G. R. Odette and B. L. Chao, unpublished notes.